Biosensors and Bioelectronics 92 (2017) 259–265

Contents lists available at ScienceDirect

Biosensors and Bioelectronics

journal homepage: www.elsevier.com/locate/bios

A reusable aptasensor of thrombin based on DNA machine employing resonance light scattering technique

Yining Hou[a], Jifeng Liu[b], Min Hong[a], Xia Li[a], Yanhua Ma[a], Qiaoli Yue[a,*], Chen-Zhong Li[c,*]

[a] Department of Chemistry, Liaocheng University, Liaocheng 252059, China
[b] Key Laboratory of Food Nutrition and Safety, Ministry of Education of China, Tianjin University of Science and Technology, Tianjin 300457, China
[c] Nanobioengineering/Bioelectronics Laboratory, Department of Biomedical Engineering, Florida International University, Miami, FL 33174, USA

ARTICLE INFO

Keywords:
Thrombin
Magnetic nanoparticles
Reusable aptasensor
Resonance light scattering

ABSTRACT

The design of molecular nanodevices attracted great interest in these years. Herein, a reusable, sensitive and specific aptasensor was constructed based on an extension-contraction movement of DNA interconversion for the application of human thrombin detection. The present biosensor was based on resonance light scattering (RLS) using magnetic nanoparticles (MNPs) as the RLS probe. MNPs coated with streptavidin can combine with biotin labeled thrombin aptamers. The combined nanoparticles composite is monodispersed in aqueous medium. When thrombin was added a sandwich structure can form on the surface of MNPs, which induced MNPs aggregation. RLS signal was therefore enhanced, and there is a linear relationship between RLS increment and thrombin concentration in the range of 60 pM–6.0 nM with a limit of detection at 3.5 pM ($3.29S_B/m$, according to the recent recommendation of IUPAC). The present aptasensor can be repeatedly used for at least 6 cycling times by heat to transfer G-quadruplex conformation to single strand of DNA sequence and release thrombin. MNPs can be captured by applying the external magnetic field. Furthermore, the proposed biosensor was successfully applied to detect thrombin in human plasma.

1. Introduction

Thrombin, an allosteric serine protease, is a key enzyme in the blood coagulation and wound healing processes. Thrombin is produced by proteolytic activation of the zymogen prothrombin. Thrombin catalyzes the conversion of fibrinogen – a soluble plasma protein – into long, sticky threads of insoluble strands of fibrin, as well as many other coagulation-related reactions. In addition to its role in blood coagulation process, thrombin involves in onset and progression of several diseases, such as antherosclerosis (Borissoff et al., 2009), pro-inflammatory cascades (Borissoff et al., 2009), and angiogenesis (Kongsuphol et al., 2014). Due to the clinical importance of thrombin, it would be tremendously valuable to establish a fast and reliable way for the detection of thrombin.

The aptamer-based thrombin sensing assay is reported as one of the common techniques in use for the detection of its presence and activity (Deng et al., 2014). Nucleic acid aptamer is a single-stranded oligonucleotide, which is completely engineered from random-sequence DNA or RNA libraries in an in vitro selection process (Ellington and Szostak, 1990). Aptamer has specific binding affinity to various targets, ranging from small inorganic and organic substances to even a protein or cell (Han et al., 2009; Luzi et al., 2003; Tuerk and Gold, 1990). For human α-thrombin (we used in this work), there are two aptamers. One is 15-mer DNA oligonucleotide (5′-GGT TGG TGT GGT TGG-3′), which was first described by Bock et al. in 1992 (Bock et al., 1992). The 15-mer thrombin aptamer interacts with one of the two anion binding sites of thrombin. The other one is 29-mer DNA oligonucleotide (5′-AGT CCG TGG TAG GGC AGG TTG GGG TGA CT-3′), which binds to the heparin-binding exosite of thrombin. The two aptamers can bind on two distinct binding sites of thrombin without interfering with each other's binding. In this case, it is easy to construct a sensing method using a "sandwich" format, such as electrochemical aptasensors (Kongsuphol et al., 2014; Numnuam et al., 2008; Yuan et al., 2012; Zhuang et al., 2014), electrochemiluminescence aptasensor (Jin et al., 2015), chemiluminescence aptasensor (Jiang et al., 2014), fluorometric aptasensor (Pu et al., 2009; Xu et al., 2012; Zhao et al., 2015), fluorescence polarization aptasensor (Yue et al., 2014), colorimetric aptasensors, and surface-enhanced Raman scattering (SERS) aptasensors, and quartz crystal microbalance (QCM) (Zhang et al., 2014). Although these methods can give good selectivity and sensitivity, the reusability is not considered. In this work, a magnetic aptasensor was constructed. The present sensor can be easily controlled with free

* Corresponding authors.
E-mail addresses: yueqiaoli@yahoo.com (Q. Yue), licz@fiu.edu (C.-Z. Li).

http://dx.doi.org/10.1016/j.bios.2017.02.024
Received 8 November 2016; Received in revised form 28 January 2017; Accepted 16 February 2017

fluorescent label, and without the instability arised from fluorescent bleaching and tedious manual handling of analyte samples. Furthermore, the sensor can be repeatedly used and the whole process for the detection of analyte can be accomplished within several minutes.

Resonance light scattering (RLS) is widely used in many studies due to its high sensitivity, convenience in performance, simplicity, and rapidity, which is a process where the incident light energy is in, or close to the absorption band of the system. It is convenient to obtain the light scattering signals by synchronously scanning both the excitation and emission monochromators on a common spectrofluorometer (Pasternack et al., 1993). Owing to the strong dependence of signal intensity on the aggregation or assembly of samples, RLS based assays have been used to detect sensitively metal ions (Liu et al., 2009; Wu et al., 2010), bacteria (Huang and Chen, 2008), peptides (Wang et al., 2011) and proteins (Jiang et al., 2006; Liu et al., 2006). These methods are based on the assemblies of gold or silver nanoparticles, which are often accompanied by distinct changes in RLS signals. These methods facilitate the procedure for monitoring analytes. Furthermore, RLS can even be used in device. Taking Heier's work as an example, RLS based on manufactured dye films was firstly used in devices to investigate the process of cyanine aggregate formation in dewetting films (Tisserant et al., 2014). In this case, it is potential to build some new sensors using RLS in the application of point-of-care testing (POCT) in the future.

Magnetic nanoparticles (MNPs) have been widely used for construction of biosensing devices because of their high biocompatibility and protein load capacity (Li et al., 2010). The focus of this work is to design a novel biosensor to detect thrombin employing MNPs as a RLS probe (Scheme 1). The strategy combined the advantages of functionalized MNPs due to their magnetism for easy separation and the specific interaction between aptamer and thrombin to form sandwich structural complex. It was suitable to construct a reusable biosensor by recording the increase of RLS signal (ΔRLS) for aggregation/disaggregation of MNPs with/without thrombin with the thermo dynamic assistance in aqueous media. In presence of thrombin, it reacts with DNA sequences, thus causing MNPs aggregation due to the formation of sandwich structure, and then resulting in enhanced RLS signals (Scheme 1). When the solution was heated the sandwich structure of thrombin aptasensor was destroyed. The MNPs can be collected by applying the external magnetic field and the sensor can be reused. Furthermore, the developed technique in this work can be used for real sample analysis with high accuracy.

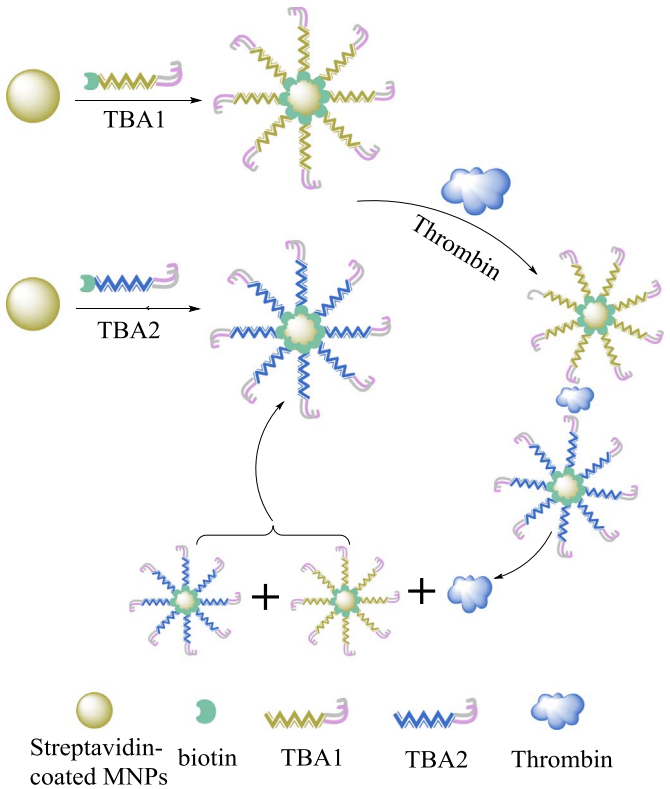

Scheme 1. Schematic representation of a magnetic aptasensor for thrombin detection.

2. Experimental section

2.1. Apparatus

All RLS measurements were carried on a LS 55 spectrofluorometer (Perkin Elmer, USA) with a 1.0 cm length sample cell. The absorption spectra were recorded using a Lambda 750 spectrophotometer (Perkin Elmer, USA) with a temperature-programmed thermo device. The digital photos were captured with Nikon 4500 digital camera (Tokyo, Japan). Transmission electron microscope (TEM) images were obtained on a JEM 2100 electron microscope with the acceleration voltage at 200 kV (JEOL Ltd., Japan), and a drop of sample suspension were placed on a carbon-coated copper grid. Dynamic light scattering (DLS) data were obtained on a Zetasizer APS instrument (Malvern, UK).

2.2. Chemicals and reagents

20, 50 and 100 nm sized iron oxide MNPs coated with streptavidin were purchased commercially (Micromod, GmbH Germany). For MNPs used in this work, 1, 2, and 10 molecules of streptavidin per particle were modified on the surface of 20, 50 and 100 nm nanoparticles, respectively, according to the product instruction. Human α-thrombin, serine, lysine, threonine, aspartate, bovine serum albumin (BSA), human serum albumin (HSA), lysozyme, and glucose oxidase (GOD) were ordered from Sigma. 15-mer thrombin aptamer labeled with biotin named TBA1 (5′-biotin-GGT TGG TGT GGT TGG-3′) and 29-mer aptamer labeled with biotin named TBA2 (5′-AGT CCG TGG TAG GGC AGG TTG GGG TGA CT-biotin-3′) were synthesized and purified by Shanghai Sangon Biotechnology Co., Ltd. Tris (hydroxymethyl)-aminomethane (Tris), 4-(2-hydroxyethyl)piperazine-1-ethanesulfonic acid (HEPES) and 3-(N-morpholino)propanesulfonic acid (MOPs) were purchased from Fluka (Buchs, Switzerland). (Reagents for selection test) NaOAc, NaH_2PO_4, Na_2HPO_4, HOAc, HCl and other common salts used were obtained from Beijing Chemical Works (Beijing, China). All chemicals were used without further purification and deionized water (≥18.2 MΩ) was prepared using a Millipore water system.

2.3. Procedures for thrombin sensing

50 nm-sized MNPs coated with streptavidin (0.1 mg ml^{-1}) were treated directly in 10 mM HEPES solution by dilution from stock solution to 2.0 ml. There should be 8 aptamers on every particle for 50 nm-sized MNPs since there are 2 molecules of streptavidin on the surface of particle and 0.25 streptavidin monomer-biotin binding mode for the reaction of streptavidin and biotin. 5.0 nM TBA1 and 5.0 nM TBA2 were added to 1.0 ml MNPs dispersion, respectively. And then they were incubated for about 20 min at room temperature to form composite of MNPs and aptamers (denoted as MNPs@TBA1 and MNPs@TBA2, respectively). To the mixture of the dispersions of MNPs@TBA1 and MNPs@TBA2, a series of thrombin standard solutions (60 pM–6.0 nM thrombin) were added to form MNPs@TBA1–thrombin–MNPs@TBA2.

Stock solutions of other biological species such as serine, lysine, threonine, aspartate, BSA, HSA, lysozyme, and GOD used for interference study were prepared in water with a similar procedure. Briefly,

100 μg ml^{-1} MNPs, 5.0 nM TBA1, 5.0 nM TBA2 were mixed to form MNPs@TBA1 and MNPs@TBA2, respectively. Subsequently, 1.0 nM thrombin was added to the mixture of MNPs@TBA1 and MNPs@TBA2, and the RLS intensity was recorded. By comparison, 1.0 nM thrombin was substituted by 1.0 μM interfering species with RLS readout.

The RLS spectra were recorded by scanning simultaneously the excitation and emission monochromators of the spectrofluorometer in the wavelength range of 200.0–700.0 nm, with same starting wavelength (Δλ =0 nm) and scanning speed. In the procedure, the slits of both the excitation and emission monochromators were kept at 2.5 nm. RLS intensity was measured at 406.0 nm.

2.4. Pretreatment of plasma samples

Fibrinogen should be precipitated firstly from plasma samples to avoid sample clotting. The procedure for pretreatment of plasma samples was referred to the literature (Chen et al., 2010). Briefly, 1.25 ml NH_4SO_4 (2 M) and 1 ml NaCl (0.1 M) were added to 0.25 ml plasma sample, the mixture was centrifuged for 10 min after suspension of 5 min. And then the supernatant was eluted in a NAP column. The content of protein in plasma and eluted sample can be evaluated by spectroscopy method, and the loss of protein can be monitored after fibrinogen precipitation. The proteolytic processing was employed for the conversion of prothrombin to thrombin, since thrombin in plasma is in the form of prothrombin. For the generation of thrombin 0.03 M $CaCl_2$ was added to the plasma sample without fibrinogen, which was detected *via* the proposed aptasensor.

3. Results and discussion

3.1. Principle for thrombin aptasensor

The present work is mainly based on the combination of thrombin and aptamer and the use of MNPs. The G-rich DNA of TBA1 and TBA2 labeled with biotin can be immobilized on the streptavidin functionalized MNPs (MNPs@TBA1 and MNPs@TBA2) through the specific interaction between streptavidin and biotin (Scheme 1). The combined nanoparticles composites including MNPs@TBA1 and MNPs@TBA2 are monodispersed in the aqueous medium (as shown in TEM images of Fig. 1). When thrombin is added to the system, thrombin can react with DNA sequences to form MNPs@TBA1–thrombin–MNPs@TBA2. MNPs aggregated due to the conformation of G-quadruplex structure and the formation of thrombin aptamers sandwich complexes, which resulted in enhanced RLS signals, as schematically illustrated in Scheme 1. To obtain the reusability of the present sensor, conformational transitions of TBA1 and TBA2 sequences were used based on a reversible equilibrium between a G-quadruplex structure and a relaxable single strand. The transition between these two conformational states was accelarated by heat, which was investigated in prior work (Alberti and Mergny, 2003) (Scheme 1).

(1) Use of MNPs. In comparison with metal nanoparticles, MNPs are easy to prepare and have low toxicity (Colombo et al., 2012). Moreover, their magnetism makes the biosensors construction steps much easier by application of an external magnetic field. Functionalized MNPs, composed of both inorganic and organic components, have recently been examined as promising platforms for detection and separation (Jung et al., 2011). For example, 4,4-difluoro-4-bora-3a-4a-diaza-s-indacene (BODIPY) functionalized-Ni@SiO_2 core/shell nanoparticles are employed as chromogenic sensors for lead ions (Lee et al., 2009), similarly nitrobenzofurane-functionalized Ni@SiO_2 core/shell MNPs are applied to detect and separate copper ion (Cu^{2+}) (Park et al., 2010b), furthermore, the amino-naphthalimide-functionalized Fe_3O_4@SiO_2 core/shell MNPs are used for the detection and separation of mercury and methylmercury ions (Park et al., 2010a). MNPs can also be modified by biomolecules so as to take the advantage of specific binding to detect or purify the biological entities. In this work, as a carrier for thrombin aptamer, MNPs were employed as RLS probes.

(2) Binding of streptavidin and biotin. Interactions between biomolecular pairs with specific affinity exist prevailingly in nature. The binding between streptavidin and biotin has long been regarded as the strongest noncovalent biological interaction, with the highest known affinity (Ka ≈10^{15} M^{-1}). This bond forms very rapidly and is stable in wide ranges of pH and temperature (Savage et al., 1992; Tong and Smith, 1992). Furthermore, the non-cooperativity in biotin binding to streptavidin is reported by using equilibrium binding (Jones and Kurzban, 1995) and under saturating condition the fully liganded tetrameric species (0.25 streptavidin monomer-biotin) predominated (Gonzalez et al., 1997). In addition, when used as a bridge the binding reaction between streptavidin and biotin is stable enough at the mild temperature of 50 °C (Pontani et al., 2012) and even 60 °C (Hadorn et al., 2012). In fact, it was reported that the interaction of streptavidin and biotin can break above 70 °C without denaturing the streptavidin tetramer, in which biotin and streptavidin remained active after dissociation and can be reused (Holmberg et al., 2005). The high affinity of the noncovalent interaction between streptavidin and biotin forms the basis for the formation of an irreversible and specific linkage between biological macromolecules.

(3) Formation of TBA1-thrombin-TBA2 complexes. For the two aptamers, the 15-mer TBA1 binds to the fibrinogen-binding site of thrombin, with a dissociation constant (K_d) of ~100 nM (Tasset et al., 1997), and the 29-mer TBA2 has a higher binding affinity, and it binds to the heparin-binding site of thrombin (K_d ~0.5 nM) (Tasset et al., 1997). As reported by the previous results of NMR (Marathias and Bolton, 2000; Schultze et al., 1994) and X-ray (Padmanabhan et al., 1993) experiments, TBA1 forms two planar G-quartets along with two TT-loops and one TGT-loop. In particular, the TT-loops play a role in specific binding with the serine protease thrombin during the blood coagulation process (Nagatoishi et al., 2011). Furthermore, the TGT-loop in the middle of the aptamer sequence interacts with the upper quadruplex plane of the native state and increases the stability of G-quadruplexes (Mao and Gmeiner, 2005).

In the strategy, 50 nm streptavidin functionalized MNPs were employed as RLS probes. In the presence of thrombin, TBA1 and TBA2 DNA sequences linked together with thrombin as the filling of sandwich, which induced aggregating behavior of MNPs (Scheme 1). Due to the complex interaction of thrombin and aptamers, the aggregation/disaggregation of MNPs@TBA1–thrombin–MNPs@TBA2 results in the significant RLS signal change. TEM images (Fig. 1), digital photos (Fig. S1, shown in Supplementary material) and Dynamic Light Scattering (DLS) data (Figs. S2–S4 shown in Supplementary material) can verify that MNPs@TBA1–thrombin–MNPs@TBA2 formed and MNPs aggregated in the presence of thrombin.

It was known that the light scattering intensity (I) could be calculated with the Rayleigh scattering law when the size of a single particle was 20-fold smaller than the wavelength of incident light beam (Yguerabide and Yguerabide, 1998a, 1998b).

$$I = \frac{8\pi^4 a^6 n_{med}^4 I_0}{r^2 \lambda_0^4} \left| \frac{m^2 - 1}{m^2 + 2} \right|^2 (1 + \cos^2\theta) \quad (1)$$

In Eq. (1), a is the particle radius, n_{med} is the refractive index of the medium surrounding the particle, I_0 is the intensity of incident monochromatic light, r is the distance between the particle and the position where the scattered light is detected, λ_0 is the wavelength of

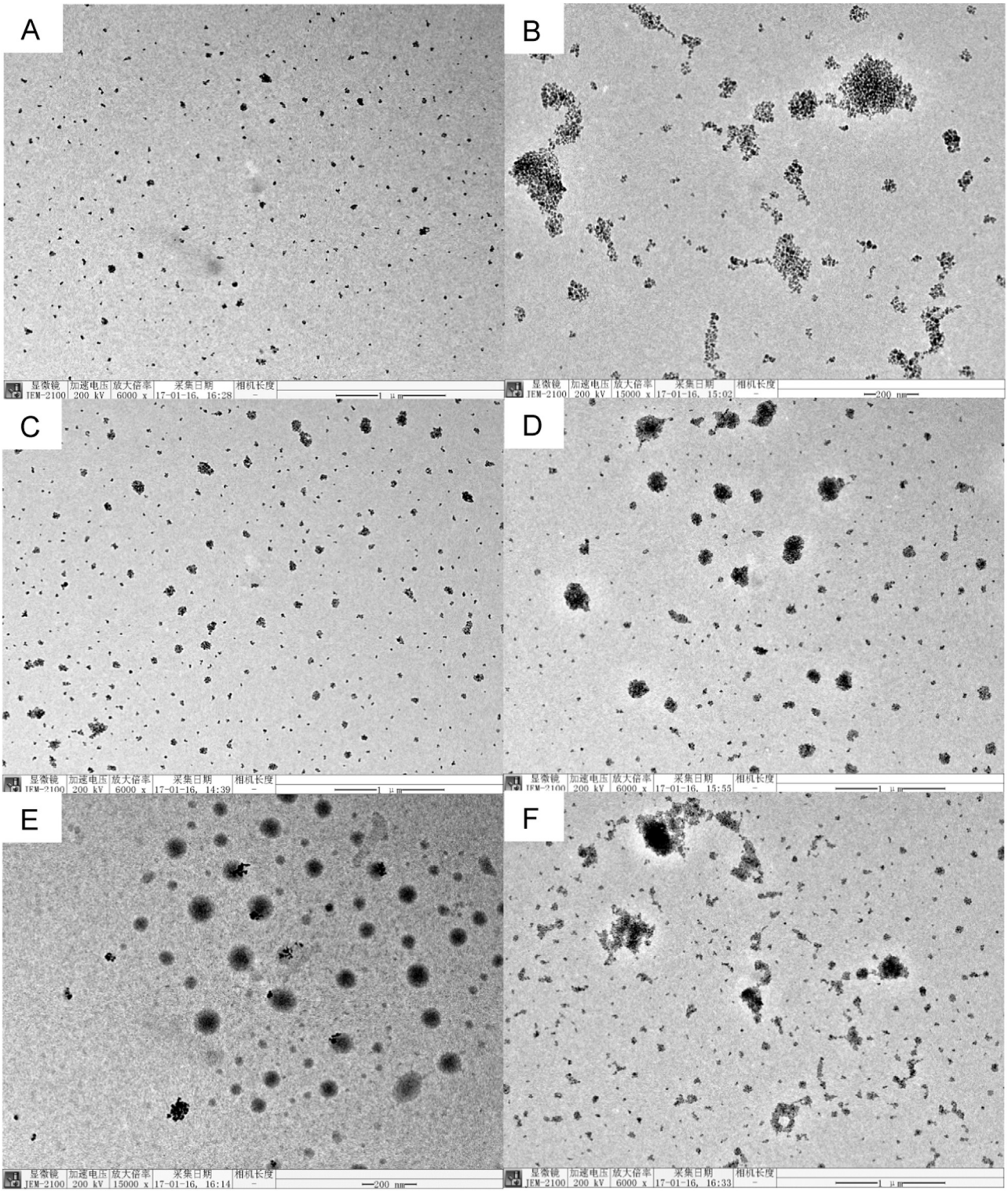

Fig. 1. TEM images of MNPs@TBA1 and MNPs@TBA2 for 20 nm (A), 50 nm (C), and 100 nm MNPs (E) system and the responsive aggregation induced by 30 nM thrombin (B, D and F), respectively. The scale bars were 1 μm for A, C, D, and F, and 200 nm for B and E. MNPs 100 μg ml^{-1}.

light in vacuum, m is the relative refractive index of the bulk particle material, and θ is the angular distribution of scattered light intensity. However, the aggregated MNPs are too big with diameters and much greater than 1/20 of the light wavelength, the light scattering properties do not obey Rayleigh's equation (Yguerabide and Yguerabide, 1998a, 1998b). In addition, the aggregation species are not homogeneous and then it is also hard to explain their light scattering behavior using Mie theory (Liu et al., 2009; Yguerabide and Yguerabide, 1998a, 1998b).

3.2. Optimization of conditions

To optimize the conditions, the influence of MNPs' size and concentration, buffer composition and pH (as shown in Supplementary material), reaction time and biotin labeled DNA concentration (Supplementary material), and temperature for reusability

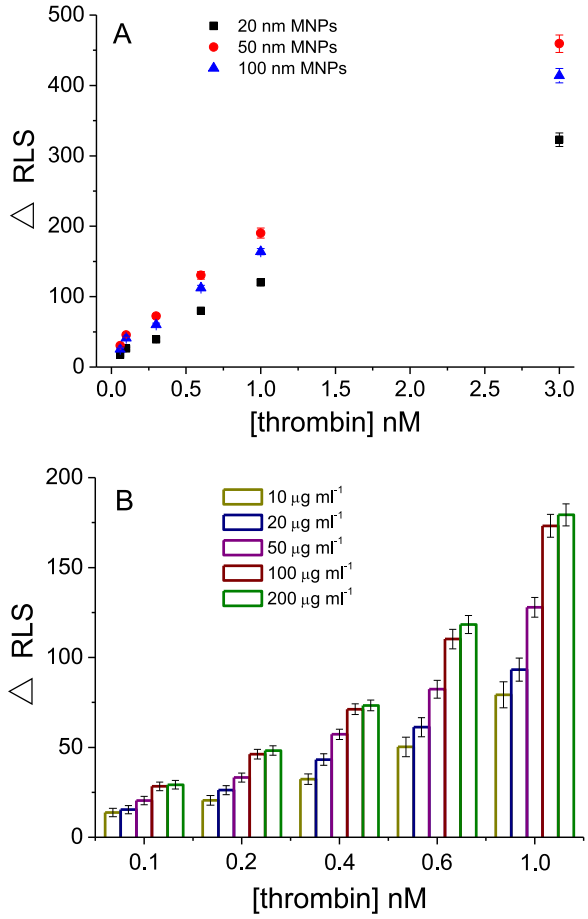

Fig. 2. Effect of MNPs' size (A) and concentration (B) on the enhancement of RLS signal in the presence of 60 pM–3.0 nM and 0.1–1.0 nM thrombin.

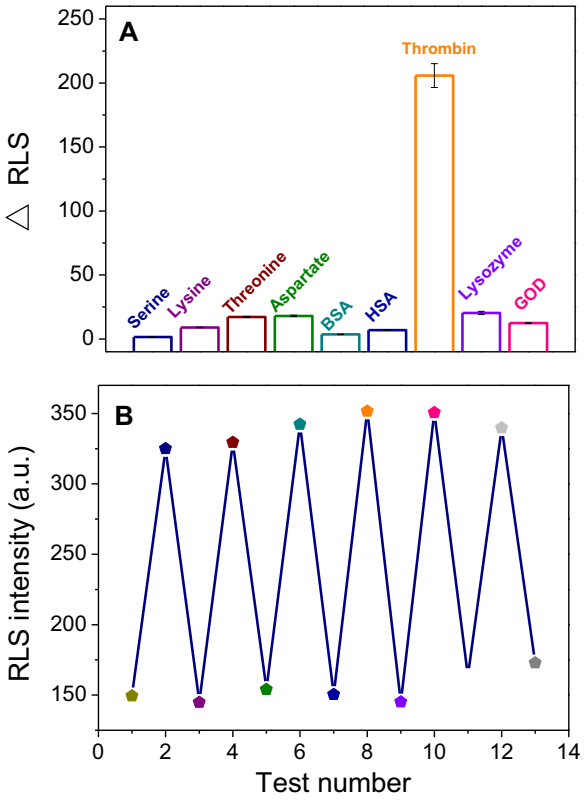

Fig. 3. Selectivity (A) tested with the ΔRLS in the presence of different amino acids and proteins, and reusability (B) investigated by comparison of the RLS intensity for MNPs@ aptamer with 1.0 nM thrombin and recovered by the assistance of heat and external magnetic field. The error bars were obtained from three separate measurements with RSD less than 5.0%. Conditions: 100 μg ml^{-1} MNPs, 5.0 nM TBA1, 5.0 nM TBA2, and 1.0 μM other protein and amino acids.

(Supplementary material) were investigated.

3.2.1. Effect of MNPs

It is known that the aggregation state of nanoparticles changes with their concentrations as well as their size. The influences of size and concentration of MNPs were studied since MNPs were appointed as the RLS probes. Herein, 20, 50, and 100 nm MNPs were employed to test the effect of MNPs size on the detection of thrombin. To confirm the aggregation/disaggregation of the MNPs with and without thrombin, TEM images for all tested MNPs including 20, 50 and 100 nm MNPs were shown in Fig. 1, and DLS was also carried out (Figs. S2–S4 in Supplementary material). It can be observed that, for all sized MNPs tested, the aggregation is evident and the size change is obvious for MNPs after thrombin addition. In addition, it was found that the size increase of MNPs is largest for 50 nm nanoparticles among 20, 50, 100 nm-sized MNPs. In addition, the linear responses of the relative RLS intensity versus [thrombin] were made using 20, 50 and 100 nm MNPs, respectively, with thrombin in the range of 60 pM–3.0 nM. As illustrated in Fig. 2A, it can be seen that the responses of RLS intensity to [thrombin] were all in a good linearity for the system using 20, 50 and 100 nm MNPs. Furthermore, the sensitivity for thrombin detection using 50 nm MNPs was higher than those of 20 and 100 nm MNPs (due to the larger slope value).

10, 20, 50, 100 and 200 μg ml^{-1} MNPs were used to study the effect of MNPs' concentration. In the procedure, ΔRLS was recorded after addition of 0.1, 0.2, 0.4, 0.6 and 1.0 nM thrombin using the five MNPs samples, respectively (Fig. 2B). It can be observed that ΔRLS increased with increasing thrombin concentration ([thrombin]). In addition, the difference of ΔRLS was not significant for the system using 100 and 200 μg ml^{-1} MNPs when the concentration of thrombin was more than 0.4 nM. Considering the highest ΔRLS as well as the least of reagent waste, 100 μg ml^{-1} MNPs was used for the following experiments.

3.3. Specificity and reusability

In this experiment, some biological species including amino acids like serine, lysine, threonine, and aspartate, and protein such as BSA, HSA, lysozyme, and GOD were selected to investigate the specificity of the present RLS aptasensor. In a typical experiment, the RLS aptasensor was incubated with 1.0 nM thrombin, 1.0 μM serine, lysine, threonine, aspartate, BSA, HSA, lysozyme, and GOD in HEPES buffer solution, respectively. As Fig. 3A showed, RLS signal of the present system changed less for amino acids and other proteins, while a significant RLS increase was observed for thrombin. It indicated from Fig. 3A that the present aptasensor showed good selectivity for thrombin determination rather than common amino acids and proteins.

As nanomachine models the duplex-quadruplex (Alberti and Mergny, 2003) and the single-strand-quadruplex (Mergny and Maurizot, 2001) equilibrium reactions were studied, respectively, in which the interconversion between duplex or single-strand and quadruplex topological states was caused by increasing temperature. Based on the transition of G-rich DNA sequence from G-quadruplex structure to relaxable single strand, the present aptasensor can be reused many cycling times. Heat was used in the experiment to accelerate the transition of DNA conformation. The solution of MNPs@ TBA1–thrombin–MNPs@TBA2 was incubated in water bath with the temperature of 50 °C as described in Section S1.1 (in Supplementary material). The G-quadruplex structures of TBA1 and TBA2 were destroyed quickly due to increase of temperature and then thrombin

was released. MNPs connected with probe DNA were collected by applying an external magnetic field. Based on the formation of TBA1-thrombin-TBA2 complexes between probe DNA labeled on the surface of MNPs and thrombin, MNPs aggregated together and then RLS intensity was enhanced. When the system was heated the quadruplex structural DNA sequence converted to single-stranded one. Corresponding to the procedure of MNPs disaggregation and redispersion, RLS signal can increase and return the background as shown in Fig. 3B. Folding of the probe DNA was also confirmed using ultra-violet (UV) absorption and UV melting experiments (data not shown).

3.4. Stability and sensitivity

Before the testing of sensitivity, the stability of the aptasensor was investigated, and it showed that the RLS intensity remained almost unchanged for several days after reaction. Furthermore, if the present sensor was heated, it was important to select an optimum temperature. On one hand heat can accelerate the transition of aptamer conformation; on the other hand high temperature can possibly destroy the binding of streptavidin and biotin. Thus, the effect of temperature on the stability of the proposed aptasensor was also investigated employing absorption and RLS methods as described in Section S2.4 of Supplementary material. From Fig. S8 (in Supplementary material), it can be found that the optimum temperature was 50 °C.

Under the optimum conditions such as 100 μg ml^{-1} MNPs, 5.0 nM TBA1, 5.0 nM TBA2, and HEPES buffer with pH 6.0, different concentrations of thrombin were detected. RLS signal was enhanced with the increasing concentration of thrombin (Fig. 4). ΔRLS was response linearly to thrombin's concentration in the range of 60 pM–6.0 nM, with the equation of ΔRLS=138.316C+29.962 (R^2=0.9924). According to the criterion of IUPAC recommendation, the detection limit of thrombin can be calculated as 3.5 pM from $3.29S_B/m$. In this equation, S_B and m were the standard deviation of the blank (n=11) and the slope of the linear calibration curve, respectively. The limit of detection (LOD) of the present aptasensor for thrombin was lower than those of previous reports (Wang and Liu, 2009; Yue et al., 2014).

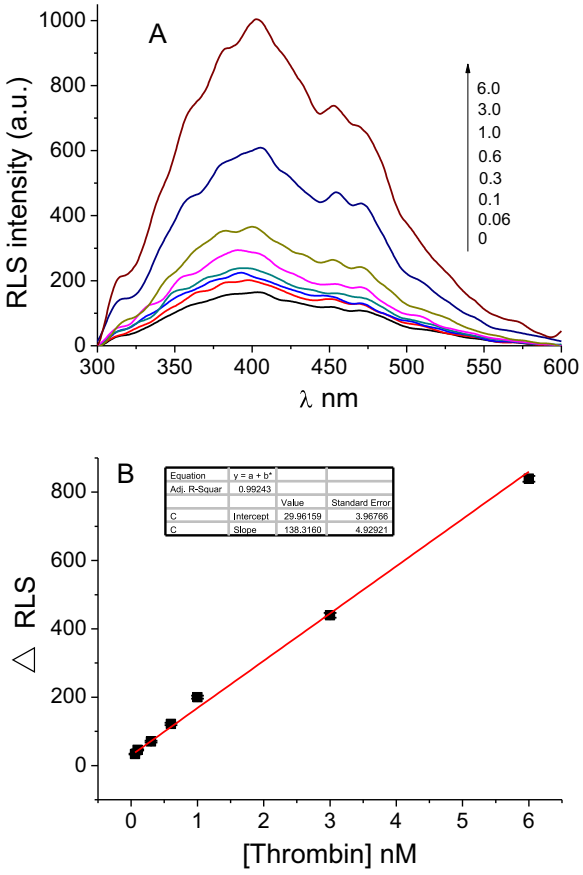

Fig. 4. RLS spectra (A) and linear response (B) of the present biosensor for thrombin in the range of 60 pM–6.0 nM. The RLS intensity was recorded at 406.0 nm for B. The error bars were obtained from three separate measurements with RSD less than 4.0%. Conditions: 100 μg ml^{-1} MNPs, 5.0 nM TBA1, 5.0 nM TBA2.

3.5. Thrombin detection in human plasma

Enzyme-linked immunosorbent assay (ELISA) is widely used for thrombin analysis in plasma in clinical tests, in which the sandwich principle and appropriate antibodies should be used. Standardized procedures are expensive, and not all the proteins have a corresponding antibody/antigen, which highlights the need for a low cost and targeted detection methodology (Chen et al., 2010). Aptamers offer several advantages over antibodies as they can be completely engineered in vitro, produced and labeled by chemical synthesis, and possess good storage properties (Centi et al., 2007; O'Sullivan, 2002; Tombelli et al., 2005). Thus, aptasensor was widely used for the rapid screening of thrombin. Herein, the RLS-based aptasensor was employed to determine thrombin in human plasma.

As demonstrated in specificity test section, there is no effect for the proteins and amino acids investigated on the RLS response of the assay. Plasma is tested after pretreatment in order to avoid clotting, fibrinogen in plasma samples was preremoved with NH_4SO_4 precipitation as described in Experimental section. Three plasma samples from different volunteers were tested, with the results shown in Table S1 (in Supplementary material). From Table S1, the content of thrombin in plasma can be calculated as 86, 114, and 105 nM and they are all around 100 nM level, which is in a good agreement with previous works (Centi et al., 2007; Chen et al., 2010; Heyduk and Heyduk, 2005).

4. Conclusions

In summary, we constructed a reusable and sensitive aptasensor for thrombin based on DNA conformational transition using the RLS technique and MNPs as the probe. In comparison with metal nanoparticles, MNPs are easy to prepare and have low toxicity (Colombo et al., 2012). Furthermore, their magnetism makes the biosensor construction steps much easier by application of an external magnetic field. The design of the present aptasensor is to combine the advantages of functionalized MNPs and the specific interaction between aptamers (TBA1 and TBA2) and thrombin to form a sandwich structure. The MNPs modified with TBA1 and TBA2, respectively, can aggregate after the addition of thrombin. The aggregation of nanoparticles resulted in the enhancement of RLS signal. The RLS increase is linear with the concentration of thrombin with the LOD of 3.51 pM via common standard working curves. The present aptasensor was used for thrombin determination both in aqueous buffer solutions and plasma samples in the presence of excess of other proteins. The strategy has the potential application for the detection of any other analyte by labeling different aptamers or ligands on MNPs' surface and even for the potential application of POCT in the future.

Acknowledgement

The present work was financially supported by Natural Science Foundation of China (91543206), Natural Science Foundation (ZR2014BQ017, ZR2015BM024, and 2013SJGZ07) and Tai-Shan Scholar Research Fund of Shandong Province and research foundation of Liaocheng University.

Appendix A. Supplementary material

Supplementary data associated with this article can be found in the online version at http://dx.doi.org/10.1016/j.bios.2017.02.024.

References

Alberti, P., Mergny, J.-L., 2003. DNA duplex-quadruplex exchange as the basis for a nanomolecular machine. PNAS 100 (4), 1569–1573.

Bock, L.C., Griffin, C., Vermaas, E.H., Toole, J.J., 1992. Selection of single-stranded DNA molecules that bind and inhibit human thrombin. Nature 355, 564–566.

Borissoff, J.I., Spronk, H.M., Heeneman, S., Cate, tH., 2009. Is thrombin a key player in the 'coagulation-atherogenesis' maze. Cardiovasc. Res. 82, 392–403.

Centi, S., Tombelli, S., Minunni, M., Mascini, M., 2007. Aptamer-based detection of plasma proteins by an electrochemical assay coupled to magnetic beads. Anal. Chem. 79 (4), 1466–1473.

Chen, X., Liu, H., Zhou, X., Hu, J., 2010. Core-shell nanostructures for ultrasensitive detection of α-thrombin. Nanoscale 2, 2841–2846.

Colombo, M., Carregal-Romero, S., Casula, M.F., Gutiérrez, L., Morales, M.P., Böhm, I.B., Heverhagen, J.T., Prosperi, D., Parak, W.J., 2012. Biological applications of magnetic nanoparticles. Chem. Soc. Rev. 41, 4306–4334.

Deng, B., Lin, Y., Wang, C., Li, F., Wang, Z., Zhang, H., Li, X.-F., Le, X.C., 2014. Aptamer binding assays for proteins: the thrombin example—a review. Anal. Chim. Acta 837, 1–15.

Ellington, A.D., Szostak, J.W., 1990. In vitro selection of RNA molecules that bind specific ligands. Nature 346, 818–822.

Gonzalez, M., Bagatolli, L.A., Echabe, I., Arrondo, J.L.R., Argaran, C.E., Cantor, C.R., Fidelio, G.D., 1997. Interaction of biotin with streptavidin. J. Biol. Chem. 272 (17), 11288–11294.

Hadorn, M., Boenzli, E., Sørensen, K.T., Fellermann, H., Hotz, P.E., Hanczy, M.M., 2012. Specific and reversible DNA-directed self-assembly of oil-in-water emulsion droplets. PNAS 109 (50), 20320–20325.

Han, K., Chen, L., Lin, Z., Li, G., 2009. Target induced dissociation (TID) strategy for the development of electrochemical aptamer-based biosensor. Electrochem. Commun. 11 (1), 157–160.

Heyduk, E., Heyduk, T., 2005. Nucleic acid-based fluorescence sensors for detecting proteins. Anal. Chem. 77, 1147–1156.

Holmberg, A., Blomstergren, A., Nord, O., Lukacs, M., Lundeberg, J., Uhlén, M., 2005. The biotin-streptavidin interaction can be reversibly broken using water at elevated temperatures. Electrophoresis 26, 501–510.

Huang, C.Z., Chen, S.F., 2008. Quantitation and differentiation of bioparticles based on the measurements of light-scattering signals with a common spectrofluorometer. J. Phys. Chem. B 112 (37), 11785–11793.

Jiang, Z., Yang, T.T., Liu, M.Y., Hu, Y.L., Wang, J., 2014. An aptamer-based biosensor for sensitive thrombin detection with phthalocyanine@SiO_2 mesoporous nanoparticles. Biosens. Bioelectr. 53, 340–345.

Jiang, Z.L., Sun, S.J., Liang, A.H., Huang, W.X., Qin, A.M., 2006. Gold-labeled nanoparticle-based immunoresonance scattering spectral assay for trace apolipoprotein AI and apolipoprotein B. Clin. Chem. 52 (7), 1389–1394.

Jin, G.X., Wang, C.M., Yang, L.L., Li, X.J., Guo, L.H., Qiu, B., Lin, Z.Y., Chen, G.N., 2015. Hyperbranched rolling circle amplification based electrochemiluminescence aptasensor for ultrasensitive detection of thrombin. Biosens. Bioelectron. 63, 166–171.

Jones, M.L., Kurzban, G.P., 1995. Noncooperativity of biotin binding to tetrameric streptavidin. Biochemistry 34 (37), 11750–11756.

Jung, J.H., Lee, J.H., Shinkai, S., 2011. Functionalized magnetic nanoparticles as chemosensors and adsorbents for toxic metal ions in environmental and biological fields. Chem. Soc. Rev. 40, 4464–4474.

Kongsuphol, P., Aryan, S.K., Wong, C.C., Polla, L.J., Park, M.K., 2014. Coiled-coil peptide based sensor for ultra-sensitive thrombin detection. Biosens. Bioelectron. 55, 26–31.

Lee, H.Y., Bae, D.R., Park, J.C., Song, H., Han, W.S., Jung, J.H., 2009. A selective fluoroionophore based on BODIPY-functionalized magnetic silica nanoparticles: removal of Pb^{2+} from human blood. Angew. Chem. Int. Ed. 48 (7), 1239–1243.

Li, D., Teoh, W.Y., Gooding, J.J., Selomulya, C., Amal, R., 2010. Functionalization strategies for protease immobilization on magnetic nanoparticles. Adv. Funct. Mater. 20 (11), 1767–1777.

Liu, S.P., Yang, Z., Liu, Z.F., Kong, L., 2006. Resonance Rayleigh-scattering method for the determination of proteins with gold nanoparticle probe. Anal. Biochem. 353 (1), 108–116.

Liu, Z.D., Li, Y.F., Ling, J., Huang, C.Z., 2009. A localized surface plasmon resonance light-scattering assay of mercury (II) on the basis of Hg^{2+}-DNA complex induced aggregation of gold nanoparticles. Environ. Sci. Technol. 43, 5022–5027.

Luzi, E., Minunni, M., Tombelli, S., Mascini, M., 2003. New trends in affinity sensing: aptamers for ligand binding. Trends Anal. Chem. 22 (11), 810–818.

Mao, X.A., Gmeiner, W.H., 2005. NMR study of the folding unfolding mechanism for the thrombin-binding DNA aptamer d(GGTTGGTGTGGTTGG). Biophys. Chem. 113, 155–160.

Marathias, V.M., Bolton, P.H., 2000. Structures of the potassium saturated, 2:1, and intermediate, 1:1, forms of a quadruplex DNA. Nucleic Acids Res. 28, 1969–1977.

Mergny, J.-L., Maurizot, J.-C., 2001. Fluorescence resonance energy transfer as a probe for g-quartet formation by a telomeric repeat. ChemBioChem 2 (2), 124–132.

Nagatoishi, S., Isono, N., Tsumoto, K., Sugimoto, N., 2011. Loop residues of thrombin-binding DNA aptamer impact Gquadruplex stability and thrombin binding. Biochimie 93, 1231–1238.

Numnuam, A., Chumbimuni-Torres, K.Y., Xiang, Y., Bash, R., Thavarungkul, P., Kanatharana, P., Pretsch, E., Wang, J., Bakker, E., 2008. Aptamer-based potentiometric measurements of proteins using ion-selective microelectrodes. Anal. Chem. 80 (3), 707–712.

O'Sullivan, C.K., 2002. Aptasensors-the future of biosensing. Anal. Bioanal. Chem. 372, 44–48.

Padmanabhan, K., Padmanabhan, K.P., Ferrara, J.D., Sadler, J.E., Tulinsky, A., 1993. The structure of α-thrombin inhibited by a 15-mer single-stranded DNA aptamer. J. Biol. Chem. 268, 17651–17654.

Park, M., Seo, S., Lee, I.S., Jung, J.H., 2010a. Ultraefficient separation and sensing of mercury and methylmercury ions in drinking water by using aminonaphthalimide-functionalized Fe_3O_4@SiO_2 core/shell magnetic nanoparticles. Chem. Commun. 46, 4478–4480.

Park, M., Seo, S., Lee, S.J., Jung, J.H., 2010b. Functionalized Ni@SiO_2 core/shell magnetic nanoparticles as a chemosensor and adsorbent for Cu^{2+} ion in drinking water and human blood. Analyst 135, 2802–2805.

Pasternack, R.F., Bustamante, C., Collings, P.J., Giannetto, A., Gibbsl, E.J., 1993. Porphyrin assemblies on DNA as studied by a resonance light-scattering technique. J. Am. Chem. Sot. 115, 5393–5399.

Pontani, L.-L., Jorjadze, I., Viasnoff, V., Brujic, J., 2012. Biomimetic emulsions reveal the effect of mechanical forces on cell-cell adhesion. PNAS 109 (25), 9839–9844.

Pu, F., Huang, Z., Hu, D., Ren, J., Wang, S., Qu, X., 2009. Sensitive, selective and label-free protein detection using a smart polymeric transducer and aptamer/ligand system. Chem. Commun. 47, 7357–7359.

Savage, D., Mattson, G., Desai, S., Nielander, G., Morgensen, S., Conklin, E., 1992. Avidin-biotin Chemistry: A Handbook. Pierce Chemical Company, Rockford, IL, 1–23.

Schultze, P., Macaya, R.F., Feigon, J., 1994. Three-dimensional solution structure of the thrombin-binding DNA aptamer d-(GGTTGGTGTGGTTGG). J. Mol. Biol. 235, 1532–1547.

Tasset, D.M., Kubik, M.F., Steiner, W., 1997. Oligonucleotide inhibitors of human thrombin that bind distinct epitopes. J. Mol. Biol. 272, 688–698.

Tisserant, J.-N., Brönnimann, R., Hany, R., Jenatsch, S., Nüesch, F.A., Mezzenga, R., Bona, G.-L., Heier, J., 2014. Resonance light scattering in dye-aggregates forming in dewetting droplets. ACS Nano 8 (10), 10057–10065.

Tombelli, S., Minunni, M., Mascini, M., 2005. Analytical applications of aptamers. Biosens. Bioelectron. 20 (12), 2424–2434.

Tong, X.C., Smith, M.L., 1992. Solid-phase method for the purification of DNA sequencing reactions. Anal. Chem. 64 (22), 2672–2677.

Tuerk, C., Gold, L., 1990. Systematic evolution of ligands by exponential enrichment: RNA ligands to bacteriophage T4 DNA polymerase. Science 249 (4968), 505–510.

Wang, C.K., Liu, D.J., Wang, Z.X., 2011. Resonance light scattering as a powerful tool for sensitive detection of b-amyloid peptide by gold nanoparticle probes. Chem. Commun. 47, 9339–9341.

Wang, Y., Liu, B., 2009. Conjugated polyelectrolyte-sensitized fluorescent detection of thrombin in blood serum using aptamer-immobilized silica nanoparticles as the platform. Langmuir 25 (21), 12787–12793.

Wu, T., Liu, C., Tan, K.J., Hu, P.P., Huang, C.Z., 2010. Highly selective light scattering imaging of chromium (III) in living cells with silver nanoparticles. Anal. Bioanal. Chem. 397 (3), 1273–1279.

Xu, B., Zhao, C., Wei, W., Ren, J., Miyoshi, D., Sugimotob, N., Qu, X., 2012. Aptamer carbon nanodot sandwich used for fluorescent detection of protein. Analyst 137 (23), 5483–5486.

Yguerabide, J., Yguerabide, E.E., 1998a. Light-scattering submicroscopic particles as highly fluorescent analogs and their use as tracer labels in clinical and biological applications I: theory. Anal. Biochem. 262, 137–156.

Yguerabide, J., Yguerabide, E.E., 1998b. Light-scattering submicroscopic particles as highly fluorescent analogs and their use as tracer labels in clinical and biological applications II. Experimental characterization. Anal. Biochem. 262, 157–176.

Yuan, Y., Yuan, R., Chai, Y., Zhuo, Y., Ye, X., Gan, X., Bai, L., 2012. Hemin/G-quadruplex simultaneously acts as NADH oxidase and HRP-mimicking DNAzyme for simple, sensitive pseudobienzyme electrochemical detection of thrombin. Chem. Commun. 48, 4621–4623.

Yue, Q., Shen, T., Wang, L., Xu, S., Li, H., Xue, Q., Zhang, Y., Gu, X., Zhang, S., Liu, J., 2014. A convenient sandwich assay of thrombin in biological media using nanoparticle-enhanced fluorescence polarization. Biosens. Bioelectron. 56, 231–236.

Zhang, Z., Liu, S., Shi, Y., Zhang, Y., Peacock, D., Yan, F., Wang, P., He, L., Feng, X., Fang, S., 2014. Label-free aptamer biosensor for thrombin detection on a nanocomposite of graphene and plasma polymerized allylamine. J. Mater. Chem. B 2, 1530–1538.

Zhao, X., Li, S., Xu, L., Ma, W., Wu, X., Kuang, H., Wang, L., Xu, C., 2015. Up-conversion fluorescence "off-on" switch based on heterogeneous core-satellite assembly for thrombin detection. Biosens. Bioelectron. 70, 372–375.

Zhuang, J., He, Y., Chen, G., Tang, D., 2014. Binding-induced internal-displacement of inverted aptamer beacon: toward a novel electrochemical detection platform. Electrochem. Commun. 47, 25–28.